The BioTac as a Tumor Localization Tool

Morelle S. Arian*
SynTouch LLC
Univ. Southern California

C.Alexander Blaine†
SynTouch LLC

Gerald E. Loeb§
SynTouch LLC
Univ. Southern California

Jeremy A. Fishel‡
SynTouch LLC

ABSTRACT

Robotically-Assisted Minimally Invasive Surgery (RMIS) offers many benefits to patients, yet introduces new challenges to surgeons due to the loss of tactile feedback that would be available in open surgery. This makes many intraoperative procedures such as tumor localization or other technically intricate and delicate tasks increasingly difficult. Reestablishing the ability to feel for surgeons during RMIS would improve the quality and safety of these surgeries and facilitate conversion of many procedures requiring touch that are traditionally performed as open-surgery. In this research a biomimetic tactile sensor (BioTac, SynTouch LLC) was evaluated for localization of artificial tumors. Various signal processing techniques implementing spatial and temporal derivatives were implemented into a graphical user interface to aid in the localization of tumors when explored by a human operator. The ability of the BioTac sensor to localize tumors was compared to performance of human subjects. The BioTac sensor was found to be particularly effective for superficial tumors (3mm deep) and able occasionally to detect smaller 3mm tumors at a depth of 12mm. While human subjects were more effective at localizing most tumors, the BioTac was often able to do so at lighter forces.

Keywords: Tactile sensing, tumor palpation, minimally invasive surgery

Index Terms: Haptic devices, Remote Medicine, User studies

1 INTRODUCTION

Minimally invasive surgery, or laparoscopic surgery, is an alternative to open surgery permitting a surgeon to operate on a patient with laparoscopic tools through small incisions made in the abdomen. Robotically-assisted Minimally Invasive Surgery (RMIS) is an enhancement to this, taking advantage of robotic control algorithms to simplify the process and make control of movements more intuitive to the surgeon. The benefits of RMIS to the patient are numerous, including reduced trauma and shorter recovery times [1]. However, these procedures eliminate tactile feedback that surgeons traditionally have available during open surgery. Tactile feedback is especially important when surgeons palpate tissue. Because of this, many operations that could benefit from RMIS are still conducted in open surgery because the intraoperative localization of internal structures is difficult in RMIS [2]. In laparoscopic surgery, surgeons have been known to insert fingers into access ports for tactile feedback [3]. In RMIS, where such probing is more difficult, it is common for surgeons to rely on preoperative scans or a simultaneous endoscopy to localize tumors but this is time consuming and expensive. Lack of tactile feedback increases the length of RMIS procedures, which in turn increases both financial cost and anaesthetic morbidity. The economic argument for RMIS hinges on reduced overall morbidity and shorter hospital stays to offset the added costs of the operation itself [4]. Restoring touch to surgeons should decrease both operating time and post-operative morbidity, reduce the incidence of reexploration surgeries, and extend the benefits of RMIS to a wider range of procedures.

A variety of tactile sensor designs have been investigated for use in RMIS. The most common design implements pressure-sensitive arrays that analyze localized pressure increases on a relatively hard surface to identify a lesion [2]. A simple, compact and inexpensive four-element one-dimensional array tactile sensor was developed by Dargahi, but the one-dimensional sensor configuration requires many movements to build a pressure map of the tissue [5]. Another tactile imaging device based on piezoresistive sensors with a resolution of 1.5mm was created that builds contour maps of the stiffness of the surface of a region to detect tumorous lumps in the breast [6]. A similar 8x8 array of piezoresistive sensors was proposed by Kattavenos for the examination of the bowel for tumors, however the resulting prototype was too large for RMIS constraints [7]. A modified laparoscopic grasper with an array of 32 conductive polymer sensors was created at the Institute of Healthcare Industries in Germany [8]. The sensor's output is displayed in a color-coded map of the tissue. A limitation with the system's mechanical design is that not all the tissues are graspable.

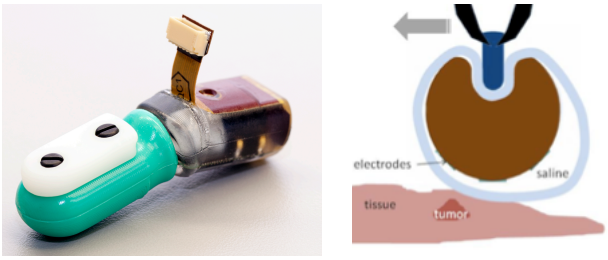

Figure 1: The BioTac (left) utilizes electrodes surrounded by a conductive liquid to measure normal and shear forces. As the BioTac slides over a surface, its elastomeric skin and the underlying liquid layer are deformed, changing the electrical resistance measured by the electrodes (right).

Most tactile sensors that have been explored measure normal forces and are insensitive to shear forces; however, the side-to-side palpation methods a doctor uses suggest that shear forces may play an important part in tumor localization. Common palpation techniques include circular motions and sliding along tissue. The BioTac (Figure 1) is a novel tactile sensor that has compliant mechanical properties similar to a human finger and is capable of similar shear force sensing. Additionally, the elastic covering of a rigid core containing sensory electrodes is very suitable for sterilization procedures that would be required in

* e-mail: morellearian@gmail.com
† e-mail: calexanderblaine@gmail.com
§ e-mail: geloeb@gmail.com
‡ e-mail: jeremyfishel@gmail.com

practical applications. In these studies the potential of the finger-sized BioTac to localize tumors is investigated. In the future, the design will be miniaturized for compliance with smaller laparoscopic ports.

2 Methods

2.1 The BioTac

The BioTac (Figure 1) emulates the finger's sensing properties by measuring skin deformation [9], [10], vibrations [11], and temperature [12]. This research utilized skin deformation, which is sensed as changes in the impedances of electrodes on the surface of a rigid core and in contact with a layer of saline injected under the silicone elastomeric skin. It has been proposed that a normal-force sensitive probe requires a sensing range on the order of 0–10N and a resolution of 0.01N to localize tumors via palpation [13]. While the BioTac possesses this sensitivity using fluid pressure [11], it cannot localize such small forces until about 30mN of force [14]. The force sensing range of the BioTac using the impedance sensing modality is 30mN to 50N.

2.2 Phantom Fabrication

A set of artificial tumor phantoms of different sizes, depths, and hardness were created in substrates of varying hardness. Other approaches to phantom tumor fabrication include silicone phantoms surrounded by a water-gelatin mixture or injecting a water-agar mixture into an ex-vivo tissue [13]. For this research, all combinations of the following parameters (except when substrate durometer was equal to tumor durometer) were used:

- Substrate Durometer: 10A and 30A
- Tumor Durometer: 30A, 40A and 60A
- Tumor Diameter: 3.18mm, 6.35mm, 12.70mm and 25.4mm
- Tumor Depth: 3mm, 6mm and 12mm

Phantom tumor models were molded from urethane rubber with a surrounding silicone "tissue" layer. The substrates were chosen because they are similar to the elasticity of soft tissue. The durometers of the phantoms were chosen because the hardness of a tumor varies qualitatively from about the hardness of a rock to a grape [2], which fall within the ranges used. A Plexiglas mold was used to create hemispherical tumor phantoms of the various diameters. These phantoms were then embedded into softer silicone at specified depths by layering silicone below and above the phantoms. A complete set of 60 phantoms was created per the specifications above in addition to two controls at each substrate durometer with no tumor phantoms. Post-curing, the specimen was coated with a small amount of KY Jelly in order to improve the lubrication of silicone and create an environment similar to what can be expected in a surgical environment.

2.3 Signal Processing

The BioTac was moved along each of the specimens by hand while electrode impedance values were recorded using a graphic user interface (GUI) available from SynTouch. The data were analyzed in Matlab to identify useful signal processing techniques. Some of the more effective visualization techniques (as discussed below) were translated into a GUI in LabVIEW for real-time feedback to the operator.

2.3.1 Temporal Derivatives

In order to enhance the saliency of the tactile signals during palpation movements, the electrode impedances were differentiated with respect to time. After differentiation the electrode readings were put through a second order Butterworth low pass filter with a cutoff frequency of 5 Hz in order to reduce noise unrelated to the slower exploratory movements. The differentiated and filtered signal was squared to enhance the signal-to-noise ratio and increase the distinction between the substrate and the tumors.

2.3.2 Spatial Derivatives

To localize the tumor, spatial derivatives were used to find the location of the phantom with respect to the electrode array. To accomplish this, the difference between two adjacent electrodes in the same plane was taken. Referring to Figure 2, electrodes positioned horizontally in a row are in the same plane. The resulting graphs were then analyzed where there was a known phantom. The electrodes in the first (1, 4, 6) and last (11, 14, 16) row and in the tip (7, 8, 9) were ignored because these points were not in contact under normal palpation. The spatial derivatives were additionally analyzed to determine whether it was possible to estimate the size of the phantom.

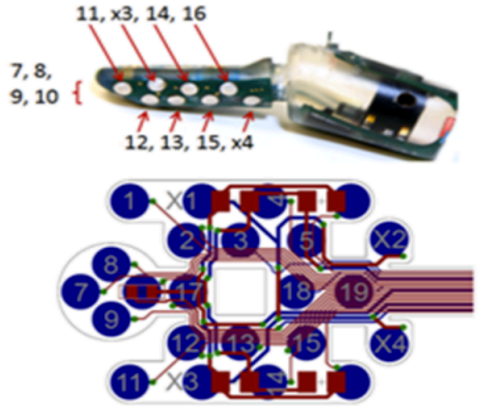

Figure 2: The BioTac electrode configuration. X's are reference electrodes; E impedances are measured with respect to the common reference electrodes.

2.4 Evaluation

Phantom detection using the BioTac was performed by the first author (M.A.), who had sufficient experience handling the BioTac and interpreting the GUI. Samples were prepared with a lubricant and placed by an assistant so they were visually occluded to the subject. The subject could freely move the BioTac and observe the GUI, but was not permitted to directly palpate the tissue. The time to localize the tumor after first contact was recorded by the assistant and a force plate (AMTI He6x6-16) measured the forces used during palpation to record the maximal force used to detect a phantom.

2.5 Comparison with Human Finger

In order to compare how the BioTac performs in contrast with a human finger, a blind study was conducted in which eight subjects without medical training were asked to use their finger(s) to palpate a specimen and indicate whether the specimen had a phantom tumor embedded within it. Prior to being blindfolded, the subjects were allowed sufficient time for training. Subjects were instructed to use whatever palpation methods they desired to accomplish the task. Each participant was timed in each trial and palpation forces were recorded using the force plate. The phantoms were classified into fourteen groups of difficulty, and one phantom was randomly selected from each group to be tested on each subject.

3 RESULTS

The results from the signal processing techniques and a comparison of human versus BioTac phantom detection abilities are described below. The averages shown for the human finger are averaged over each subject's average performance.

Average	Finger	BioTac
Accuracy	87.63 +/- 9.16%	72.48%
Force	38.76 +/- 16.70N	25.025 N
Time	14.16 +/- 3.39s	50.53 sec

Table 1: Summary of detection rate, force, and time for human finger versus BioTac. Error regions indicate standard deviations between subjects.

		Finger	BioTac
Depth	**3 mm**	87.5%	94.1%
	6 mm	87.2%	65.0%
	12 mm	83.3%	60.0%
Size	**25.4 mm**	96.6%	93.3%
	12.7 mm	96.9%	71.4%
	6.35 mm	87.0%	60.0%
	3.72 mm	62.1%	61.5%
Hardness Difference	**50A**	83.3%	63.6%
	30A	91.5%	78.3%
	20A	72.7%	83.3%
	10A	90.0%	54.5%

Table 2: The results with the human and BioTac fingers are shown in comparison to changes in phantom features. Hardness difference is calculated as the difference in durometer between the substrate and phantom.

3.1 Temporal Derivatives

The signal processing performed on the raw electrode impedances improved the saliency of the signal for detecting phantom tumors, as illustrated in Figure 3.

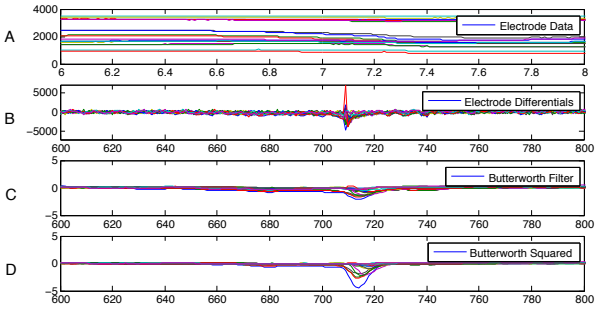

Figure 3: The BioTac was run along a 6.35mm diameter phantom of hardness 40A at a depth of 6mm embedded within silicone of hardness 10A. Graph A shows the raw electrode data. Graph B is the derivative with respect to time. C shows the derivative taken after a low pass filter was applied on the data. D is the square of the graph above it, taken to enhance signal-to-noise ratio. In D, the phantom tumor is easily distinguishable from the surrounding tissue.

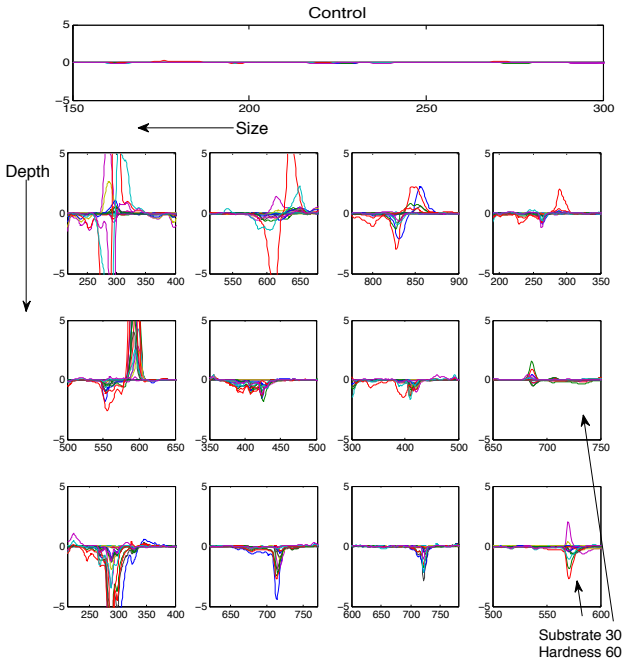

Figure 4: Substrate 10A, hardness 30A phantoms are shown. The tumors are easily distinguished from the surrounding tissue and are characterized by a spike in the derivatives. Noise is minimal as can be seen by the control (top). Substrate 30A, hardness 60A phantoms are shown for the 3.72mm diameter at depths 6mm and 12mm because these were not detectable in the substrate 10A.

All the phantoms were detectable in the 10A hardness substrates except the smallest phantom (diameter 3.72mm) at 6 and 12mm depth. The BioTac was, however, capable of detecting these phantoms in substrate 30A. With the deeper tumors, it was helpful to move the BioTac over the tumor centered about electrode 17 (see electrode configuration in Figure 2), with an angle of about 30 degrees. It took multiple attempts to get a good orientation for the BioTac with respect to the specimen, after which clear signals were obtained.

3.2 Spatial Derivatives

The BioTac electrode configuration provided only a limited set of spatial derivatives that did not provide enough information to characterize the size of phantoms; however, the results show promise in localizing phantoms on the surface of the BioTac.

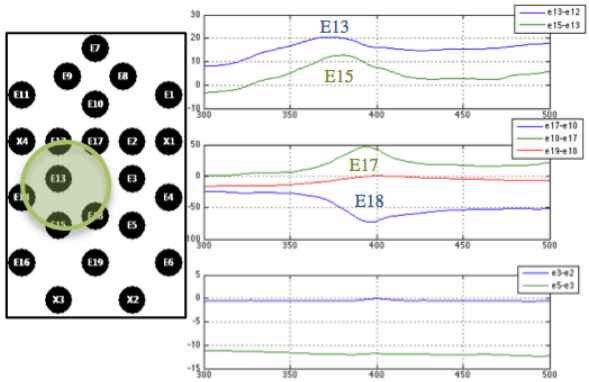

Figure 5: The spatial differential for a phantom with diameter 25.4mm, depth 6mm, hardness 40A embedded in substrate 10A. The inset left indicates the location of the phantom, and the graphs display the spatial derivatives for each plane of electrodes. This indicates that the BioTac ran over the tumor at electrodes 13, 15, 17, and 18.

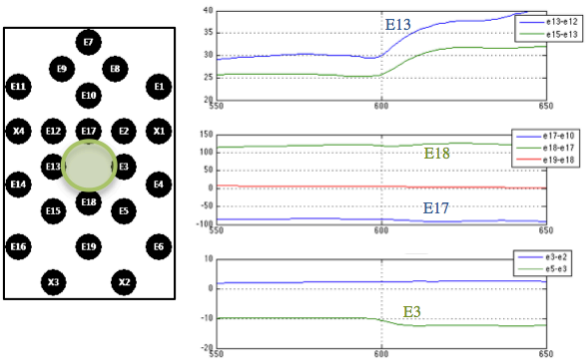

Figure 6: Spatial differential of phantom of size 3.72mm, 3mm depth, and hardness 60A in substrate 10A. The graph indicates that the phantom is located at electrodes 13, 17, 18, and 3.

The spatial derivatives were displayed in a color-coded GUI, which improved saliency as shown in the supplemental video.

3.3 Human Study

Table 1 shows that the smaller phantoms were much more difficult to localize than the larger phantoms. Perhaps surprisingly, depth was not as important a factor as size in its effect on ability to localize the phantoms. Testing larger depths might have made a larger effect on phantom detectability. Finally, hardness of the phantom had little to no correlation with the ability to detect the phantoms. The human finger outperformed the BioTac by a small margin.

The BioTac's main difficulties were in false positives and speed. Because it takes multiple passes to detect phantoms, it took longer to localize phantoms with the BioTac than simply receiving direct tactile feedback. The BioTac falsely detected phantoms when there were none in almost all trials. When the BioTac is stroked manually along the specimen, any imperfections in the surface or changes in velocity or normal pressure can cause changes in electrode impedances that look similar to a phantom. It should be noted that the phantom models had imperfections caused by the initial studies with the human fingers, which were conducted prior to the BioTac evaluation. The control models were particularly affected because participants used more force when they were unable to detect a phantom. Thus, the controls had many fingernail marks and divets that would cause the BioTac to falsely detect a phantom. In order to prevent false phantom detection where a "phantom" was actually a model imperfection, the experimenter compared actual phantom location with the result reported by the subject.

As shown in Figure 8, subjects who used more force were able to perform the best in successfully classifying tumors. Consistently lower forces were applied to the BioTac than subjects applied with their fingers (on average, 65% less), yet still had a classification accuracy that fit the trend of the other subjects. In the Time graph, the BioTac data point is far from the trend with the human finger.

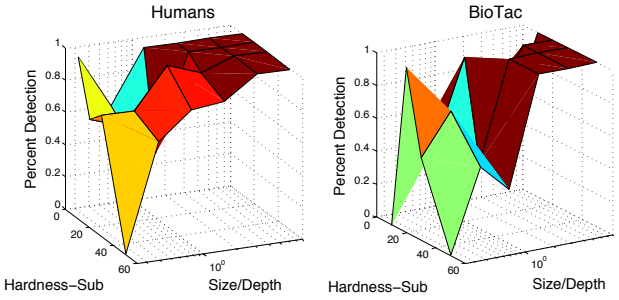

Figure 7: The human study results are shown with the percent detection of humans (right) in comparison with the BioTac (left), plotted against phantom types. For visualization purposes, the phantom factors were consolidated into two: the x-axis shows the difference in phantom and substrate hardness, and the y-axis shows the ratio of the size to depth.

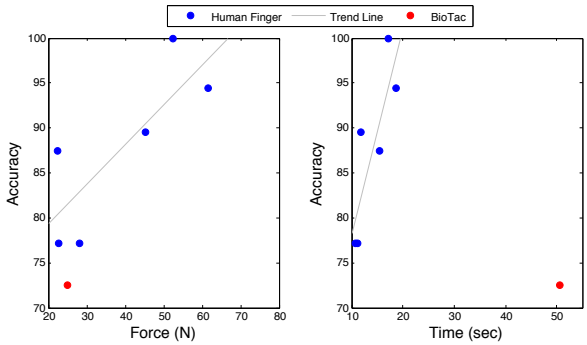

Figure 8: The above graphs show the average time and force taken by each subject (blue dots), mapped against their percent accuracy. A best-fit linear curve was drawn through the data to show the trend line. The red dot represents the percent accuracy for the BioTac.

4 Discussion

In comparison with the human finger, the BioTac was slightly inferior. The BioTac was sensitive enough to detect even the smallest surface phantom tumors tested (3.72 mm diameter, 3mm depth). Every phantom tumor except the smallest diameter tumors was detected even at the largest depth (12mm). The temporal derivatives were an effective method of localizing the phantoms. The spatial derivatives also yield useful information that can be used to find approximately where on the sensor the phantom was located. This is likely to work better with a longer array of closely spaced, coplanar electrodes. Other techniques such as normal forces can be used to further localize phantoms after initial detection.

4.1 Temporal Derivatives

The manner in which the BioTac was moved along the specimen was most important for clear results. With more difficult phantoms – smaller and deeper – multiple passes and specific orientations were needed. It was surprising that the BioTac could detect the smallest phantom in the 30A durometer substrate and not in the softer 10A durometer substrate, where the distinction between tissue and phantom hardness was larger. This is probably due to the fact that the phantom could be displaced in the softer tissue by the forces of the exploratory movement.

4.2 Spatial Derivatives

The spatial derivatives give more accurate readings with the harder, more superficial phantoms. Redesigning the electrode layout could provide more data point and reduce the noise in the spatial derivatives. The spatial differentials were not sufficient to estimate the size of the phantoms because larger tumors were not longer than the flat sensing region of the BioTac.

4.3 Normal Forces

Another effective localization technique not discussed above is utilizing the normal and tangential forces to orient the BioTac toward the phantom, as done in [2]. By equalizing opposite electrode impedances in the tip of the BioTac (electrodes 7 and 10, and 8 and 9), the normal and tangential forces could be balanced, reorienting the BioTac as necessary to preserve this balance. This strategy appeared to be effective for surface tumors when the tip of the sensor was near the edge of the phantom tumor. This exploratory technique is time consuming and is only useful when the general location of the tumor is already known and a more accurate outline is desired.

4.4 Human Study

On average, the BioTac was capable of detecting 70% of the phantom tumors, while subjects using their own fingers were able to detect 85% of the phantom tumors presented to them. The BioTac required significantly more time than the human finger, but also used less force. The major difficulty for the human finger was localizing small phantoms. The BioTac's major issue was false positives (although detecting small and deep phantoms was also difficult). The specimens, particularly the controls, were damaged in the human portion of the study, which was conducted prior to the BioTac evaluation. Fingernail marks and divets appeared to cause many false positives. Lack of visual feedback meant that it was impossible for the controller to know whether the GUI showed a phantom or an imperfection in the specimen. In an actual surgical environment, the surgeon has visual feedback, which would aid in avoiding false positives from surface features. The BioTac performed very well on very small phantoms.

On average, the BioTac was used with less force than the biological finger, but this may reflect the relatively high friction between the BioTac and the substrates despite lubrication. The friction between the BioTac and real biological tissues such as within the abdomen remains to be determined.

5 Conclusion

In the future, the BioTac will be redesigned specifically for use in surgical environments. In redesigning the BioTac, all physical characteristics must comply with RMIS standards. The BioTac will be straight and smaller in diameter to fit through typical surgical ports. It will need to be sterilizable and easily assembled and filled with saline in the operating room. The skin thickness, inflation volume and electrode configuration will be optimized for RMIS applications. This should substantially improve sensitivity and spatial resolution (currently 2mm). The fingerprint pattern on the BioTac skin will be eliminated, which should reduce vibration noise and perhaps frictional forces during sliding, as well as simplifying manufacture. A single element ultrasound transducer may be integrated into the sensor in order to provide additional information about the subsurface features.

The visual feedback method for displaying the BioTac's sensor data may not be ideal, particularly if it distracts the surgeon from the view of the surgical field. An alternative to this is tactile feedback such as the tri-axial force tactor being developed at the University of Siena, which can be worn in the fingertip, explained in detail in [15]. This tactor can produce normal and shear forces on the fingertip but does not provide spatial information. This kind of tactile feedback could be faster and more intuitive for the surgeon to understand, perhaps complementing rather than completely replacing visual feedback.

6 Acknowledgements

We wish to thank Raymond Peck and Gary Lin for their invaluable help in the fabrication and development process. A special thanks to Intuitive Surgical for their guidance and support on this project.

References

[1] A. Hamed, S. C. Tang, H. Ren, A. Squires, and C. Payne, "Advances in haptics, tactile sensing, and manipulation for robot-assisted minimally invasive surgery, noninvasive surgery, and diagnosis," … *of Robotics*, 2012.

[2] M. D. Naish, R. V. Patel, A. L. Trejos, and M. T. Perri, "Robotic Techniques for Minimally Invasive Tumor Localization," *Surgical Robotics*, 2011.

[3] M. Lee, "Tactile sensing: new directions, new challenges," *Intnl J Robotics Res*, 2000.

[4] L. S. Leddy, T. S. Lendvay, and R. M. Satava, "Robotic surgery: applications and cost effectiveness," *Open Access Surgery*, vol. 3, pp. 99–107, 2010.

[5] J. Dargahi, S. Najarian, and K. Najarian, "Development and three-dimensional modelling of a biological-tissue grasper tool equipped with a tactile sensor," *Electrical and Computer …*, 2005.

[6] P. S. Wellman, E. P. Dalton, D. Krag, K. A. Kern, and R. D. Howe, "Tactile imaging of breast masses: first clinical report.," *Arch Surg*, vol. 136, no. 2, pp. 204–208, Feb. 2001.

[7] Kattavenos, Lawrenson, Frank, Pridham, Keatch, and Cuschieri, "Force-sensitive tactile sensor for minimal access surgery.," *Minim Invasive Ther Allied Technol*, vol. 13, no. 1, pp. 42–46, Feb. 2004.

[8] S. Schostek, C.-N. Ho, D. Kalanovic, and M. O. Schurr, "Artificial tactile sensing in minimally invasive surgery - a new technical approach.," *Minim Invasive Ther Allied Technol*, vol. 15, no. 5, pp. 296–304, 2006.

[9] N. Wettels, D. Popovic, and G. E. Loeb, "Biomimetic Tactile Sensor," *Proceedings of BioMed2007*, 2007.

[10] Z. Su, J. A. Fishel, T. Yamamoto, and G. E. Loeb, "Use of tactile feedback to control exploratory movements to characterize object compliance," *Front. Neurorobot*, vol. 6, 2012.

[11] J. A. Fishel and G. E. Loeb, "Sensing tactile microvibrations with the BioTac—Comparison with human sensitivity," presented at the IEEE/RAS-EMBS International Conference on Biomedical Robotics and Biomechatronics, 2012, pp. 1122–1127.

[12] C. H. Lin, T. W. Erickson, J. A. Fishel, undefined author, N. Wettels, and G. E. Loeb, "Signal processing and fabrication of a biomimetic tactile sensor array with thermal, force and microvibration modalities," presented at the IEEE International Conference on Robotics and Biomimetics, 2009, pp. 129–134.

[13] G. L. McCreery, A. L. Trejos, and R. V. Patel, "Evaluation of force feedback requirements for minimally invasive lung tumour localization," … *Robots and Systems …*, 2007.

[14] N. Wettels and G. E. Loeb, "Haptic feature extraction from a biomimetic tactile sensor: force, contact location and curvature," presented at the IEEE International Conference on Robotics and Biomimetics, 2011, pp. 2471–2478.

[15] F. Chinello, M. Malvezzi, C. Pacchierotti, and D. Prattichizzo, "A three DoFs wearable tactile display for exploration and manipulation of virtual objects," presented at the IEEE Haptics Symposium, 2012, pp. 71–76.